การตรวจวัดเชิงสีของซีสเตอีนโดยใช้อนุภาคระดับนาโนเมตรของเงิน-ไฮดรอกซีแอพาไทต์

นางสาวเร็ทโน พราเซเทีย

วิทยานิพนธ์นี้เป็นส่วนหนึ่งของการศึกษาตามหลักสูตรปริญญาวิทยาศาสตรมหาบัณฑิต
สาขาวิชาเคมี ภาควิชาเคมี
คณะวิทยาศาสตร์ จุฬาลงกรณ์มหาวิทยาลัย
ปีการศึกษา 2560

COLORIMETRIC DETECTION OF CYSTEINE USING SILVER-HYDROXYAPATITE NANOPARTICLES

Miss Retno Prasetia

A Thesis Submitted in Partial Fulfillment of the Requirements
for the Degree of Master of Science Program in Chemistry
Department of Chemistry
Faculty of Science
Chulalongkorn University
Academic Year 2017

Thesis Title	COLORIMETRIC DETECTION OF CYSTEINE USING SILVER-HYDROXYAPATITE NANOPARTICLES
By	Miss Retno Prasetia
Field of Study	Chemistry
Thesis Advisor	Assistant Professor Fuangfa Unob, Ph.D.

Accepted by the Faculty of Science, Chulalongkorn University in Partial Fulfillment of the Requirements for the Master's Degree

.....Dean of the Faculty of Science

(Associate Professor Polkit Sangvanich, Ph.D.)

THESIS COMMITTEE

.....Chairman

(Associate Professor Vudhichai Parasuk, Ph.D.)

.....Thesis Advisor

(Assistant Professor Fuangfa Unob, Ph.D.)

.....Examiner

(Associate Professor Thumnoon Nhujak, Ph.D.)

.....External Examiner

(Assistant Professor Jinda Yeyongchaiwat, Ph.D.)

เร็ทโน พราเซเทีย : การตรวจวัดเชิงสีของซีสเตอีนโดยใช้อนุภาคระดับนาโนเมตรของเงิน-ไฮดรอกซีแอพาไทต์ (COLORIMETRIC DETECTION OF CYSTEINE USING SILVER-HYDROXYAPATITE NANOPARTICLES) อ.ที่ปรึกษาวิทยานิพนธ์หลัก: เฟื่องฟ้า อุ่นอบ, หน้า.

ซีสเตอีนเป็นกรดอะมิโนที่ประกอบด้วยซัลเฟอร์ ซึ่งมีหน้าที่เป็นสารต้านออกซิเดชันในร่างกายมนุษย์ ซีสเตอีนในปริมาณสูงเกินไปเปลี่ยนรูปเป็นซีสตีนซึ่งเป็นสาเหตุของการเกิดนิ่วในไต กระเพาะปัสสาวะ และท่อไต ดังนั้นจึงได้พัฒนาวิธีการตรวจวัดปริมาณซีสเตอีนโดยใช้หลักการรวมตัวของอนุภาคระดับนาโนของเงินบนไฮดรอกซีแอพาไทต์ (HAp) โดยศึกษาสัณฐานของไฮดรอก-ซีแอพาไทต์ และอนุภาคระดับนาโนเงิน-ไฮดรอกซีแอพาไทต์ด้วยกล้องจุลทรรศน์อิเล็กตรอนแบบส่องผ่าน ศึกษาสีที่เปลี่ยนไปของอนุภาคระดับนาโนเงิน-ไฮดรอกซีแอพาไทต์ในสารละลายซีสเตอีนที่ความเข้มข้นต่างๆ ซึ่งสามารถตรวจวัดได้ด้วยตาเปล่า รวมทั้งสามารถหาความเข้มสีของอนุภาคระดับนาโนเงิน-ไฮดรอกซีแอพาไทต์โดยใช้โปรแกรม Image-J ในโหมดสีเทา จากนั้นนำวิธีการตรวจวัดไปประยุกต์ใช้สำหรับการตรวจวัดซีลเตอีนในตัวอย่างน้ำปัสสาวะ โดยมีขั้นตอนการเตรียมตัวอย่างสำหรับการตรวจวัดโดยใช้เรซินชนิดประจุบวก นอกจากนี้มีการศึกษาปัจจัยที่ส่งผลต่อการเตรียมตัวอย่างและการตรวจวัดปริมาณซีสเตอีน ได้แก่ เวลาที่ใช้ในการสกัด, เวลาที่ใช้ในการชะสารตัวอย่าง, ความเข้มข้นของ Ca^{2+} ที่ใช้เป็นตัวชะสารตัวอย่าง, การเติม NaOH, ปริมาตรในการชะสารตัวอย่าง, เวลาในการเกิดปฏิกิริยาระหว่างอนุภาคเงินกับไฮดรอกซีแอพา-ไทต์และปริมาตรของโซเดียมโบโรไฮไดรด์ พบว่าวิธีการตรวจวัดมีช่วงการตรวจวัดตั้งแต่ 0-105 μM จากนั้นใช้วิธีการเติมสารมาตรฐานในการวิเคราะห์ปริมาณของซีลเตอีนในตัวอย่างปัสสาวะ พบว่ามีค่าการวิเคราะห์กลับคืน (%recovery) ในช่วง 93.0-111.9% และส่วนเบี่ยงเบนมาตรฐานสัมพัทธ์ (% RSD) ในช่วง 1.4-6.9% วิธีการตรวจวัดมีความจำเพาะต่อซีลเตอีนเมื่อเทียบกับกรดอะมิโนชนิดอื่นที่พบในปัสสาวะ เช่น โฮโมซีสทีน, เมไธโอนีน และซีสทีน

ภาควิชา เคมี ลายมือชื่อนิสิต .....

สาขาวิชา เคมี ลายมือชื่อ อ.ที่ปรึกษาหลัก .....

ปีการศึกษา 2560

5872038923 : MAJOR CHEMISTRY

KEYWORDS: CYSTEINE; HYDROXYAPATITE; SILVER NANOPARTICLE; COLORIMETRIC DETECTION

RETNO PRASETIA: COLORIMETRIC DETECTION OF CYSTEINE USING SILVER-HYDROXYAPATITE NANOPARTICLES. ADVISOR: ASST. PROF. FUANGFA UNOB, Ph.D., pp.

Cysteine is a sulphur-containing amino acid that acts as an effective antioxidant in human body. An excessive amount of cysteine leads to cystine formation that causes the stone formation in kidney, bladder, and ureters. A new method was developed for detection of cysteine in urine samples based on the aggregation of silver nanoparticles (AgNPs) on Hydroxyapatite (HAp) in the presence of cysteine. Transmission Electron Microscope (TEM) was used to observe the morphology of prepared HAp and AgNPs on HAp. The presence of cysteine of different concentrations resulted in different cluster sizes of AgNPs on HAp and hence different solid color. The color of the AgNPs containing HAp was observed by naked eyes and the color intensity was measured by the Image J software. To detect cysteine in urine sample, a sample preparation by extraction on cation exchange resin was introduced. The parameters affecting the analysis including extraction and elution time, concentration of Ca^{2+} eluent solution, addition of NaOH, eluted sample volume, contact time between Ag^{+} and HAp, concentration of Ag^{+}, and volume of $NaBH_4$ were optimized. The working range of this method was in a range from 0 to 105 μM. The standard addition method was applied to determine cysteine concentration in urine sample. The applicability of this method was then presented in terms of percent recovery and percent relative standard deviation (% RSD) which were in the range of 92.0 to 111.9 % and 1.4 to 6.9 %, respectively. The method exhibited a selectivity toward cysteine over amino acids commonly found in urine including homocysteine, methionine, and cystine.

Department:	Chemistry	Student's Signature	.....
Field of Study:	Chemistry	Advisor's Signature	.....
Academic Year:	2017		

ACKNOWLEDGEMENTS

Foremost, I am grateful to Allah for the good health and wellbeing that were necessary to complete my thesis. In this opportunity, I would like to express my sincere gratitude to my advisor, Assistant Professor Dr. Fuangfa Unob who has supported me to finish my thesis with her kind supervision, patience, motivation, tremendous assistance, and immense knowledges. I would also like to thank the rest of my thesis committee Associate Professor Dr. Vudhichai Parasuk, Associate Professor Dr. Thumnoon Nhujak from analytical chemistry of Chulalongkorn University, and Assistant Professor Dr. Jinda Yeyongchaiwat from inorganic chemistry of Bansomdejchaopraya Rajabhat University for their encouragement, insightful comments and suggestions that greatly improved my thesis.

I would like to express my gratitude to my parents for their love and always supporting me spiritually throughout writing this thesis, hence this thesis is dedicated for them. A special thanks to my fellow labmates, Ms. Sujinda (Mew) and Ms. Patita Salee (Milk), for helping me a lot, for spending time together in working hard before deadlines, for all the fun we have had, and for always cheered me up every time. I also thank all friends in the Environment Analysis Research Unit (EARU) Group and all those whose kind assistance, support, and friendship with me for these couple years.

Last but not the least, I gratefully acknowledge the 72nd Anniversary of His Majesty King Bhumibala Aduladeja and Top-up Scholarship, Chulalongkorn University, for providing me financial support. I would never have been able to complete my thesis without all the supports.

CONTENTS

Page

Page

Page

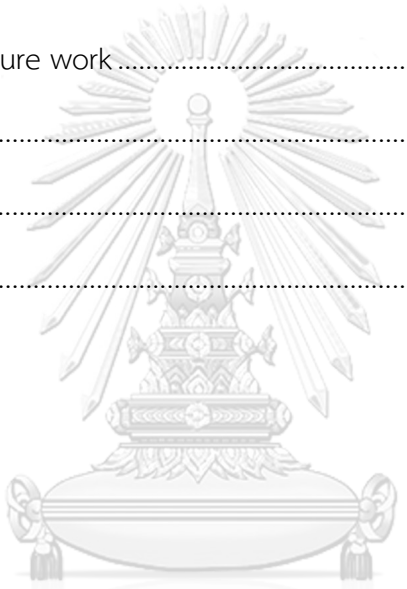

LIST OF TABLES

LIST OF FIGURES

CHAPTER I
INTRODUCTION

1.1 Statement of background and problem

Cysteine, one example of the sulphur-containing amino acids, acts as the most effective antioxidant in human body. Due to the health benefit of cysteine, it has many applications in pharmaceuticals, food and cosmetics [1]. The major function of cysteine is for determining structure of extracellular proteins by forming a disulfide bond as a bridge. The presence of the disulfide bond causes the structure of proteins more resistant against thermal condition or extreme condition [2]. The other major functions of cysteine are the precursor for glutathione and taurine synthesis, the source of sulphate and pyruvate, and the neurotransmitter.

In human body, cysteine can be produced by changing from homocysteine synthesized from methionine to cysteine or breakdown of endogenous protein [3]. Adsorption of cysteine from diets is also an alternative. Cysteine can be excreted in urine and the urinary concentration of total cysteine of the healthy individuals is in the range of 25-200 μM [4-8]. However, an excessive amount of cysteine in human body causes impaired resorption [6]. Besides that, it can also increase the possibility of cysteine oxidized form called cystine which has the solubility approximately 250 mg/L (1mM/L) [9] thus giving a risk of forming stone in kidney, bladder and ureters

which can be dissolved completely only in strong base [1]. Thus, the level of cysteine in urine can be an indicator for the disease and monitoring its urinary level.

Several methods for cysteine detection have been developed using high-performance liquid chromatography [10, 11], fluorescence spectroscopy [12], electrochemical voltammetry [13], spectrophotometry [14], and capillary electrophoresis [6, 15]. However, these methods are time consuming, expensive and sophisticated instruments. Alternatively, colorimetric methods for cysteine detection by naked eyes or by UV-Vis spectrophotometer using nanoparticles such as silver nanoparticles (AgNPs) and gold nanoparticle (AuNPs) have been studied. The latter methods were applied to detect cysteine in rat brain [16], aqueous samples [17-19], and biological fluids such as serum [20] and urine [7, 8]. The thiol group on the cysteine may form either Ag–S or Au–S bond with AgNPs or AuNPs. When a solution of salt (e.g. $Ca(NO_3)_2$, $Cu(NO_3)_2$, NaCl) was further added to interact with either amine or carboxyl group of cysteine on nanoparticles surface, the electrostatic repulsion between AuNP/cysteine or AgNP/cysteine was reduced and the aggregation of the nanoparticles occurred [4, 7, 17-20]. However, this method involved standard addition to determine the concentration of cysteine in the sample. The high sensitivity of this method was described by the value of detection limit in the range of 1-10 nM for aqueous samples [18, 19] and 0.05 μM for urine samples [8]. Previously, the use of nanoparticles has some advantages, but it still requires the use of instrument such as a UV-Vis

spectrophotometer to determine the concentration of cysteine in samples. In the present study, the use of hydroxyapatite (HAp) modified with Ag^+ as the material for colorimetric cysteine detection by naked eyes has been developed. By measuring color intensity of HAp using ImageJ software, the concentration of cysteine in the sample could be determined.

Hydroxyapatite (HAp) or $Ca_{10}(PO_4)_6(OH)_2$ was selected as solid material in this work because it is non-toxic, inexpensive and easy to synthesize [21, 22]. In the presence of other cations such of Ag^+ and K^+, Ca^{2+} on HAp could be replaced via ion exchange [23, 24]. Based on this property, in this present work, HAp was then modified with Ag^+ to be the material used for cysteine detection for onsite analysis. Moreover, the use of HAp also helps observation of a color change more obvious on a solid than that in the solution.

Colorimetric detection of cysteine is based on the aggregation of silver nanoparticles on the surface of HAp induced by the presence of cysteine and $NaBH_4$. Interaction between a thiol group of cysteine with AgNPs on HAp resulted in the formation of AgNPs clusters. The size of AgNPs cluster depends on the concentration of cysteine, and the change of material color from yellow to violet was observed in an increasing cysteine concentration. The color intensity on a solid was then observed by naked eyes and measured using the Image-J software. This method is simple and has potential in clinical screening of cysteine in urine samples.

1.2 Research objectives

The objectives of this research are as follows.

1.2.1 To develop a colorimetric method for determination of cysteine using hydroxyapatite modified with Ag^+ as the material and $NaBH_4$ as reducing agent

1.2.2 To apply the method to detect cysteine in human urine samples.

1.3 Scope of the research

The parameters affecting sample pre-treatment and detection were investigated. In the sample pre-treatment, cysteine in samples was extracted on cation exchange resin. The effects of extraction and elution time, the addition of NaOH and Ca^{2+} were studied. In the detection step using hydroxyapatite modified with Ag^+, various parameters including concentration of Ag^+, the reaction time between Ag^+ solution and HAp, sample volume, and $NaBH_4$ volume were investigated. Moreover, the matrix effect in synthetic urine and the presence of other thiol containing amino acids in the system were also examined.

Color intensity of the material was observed by naked eyes and measured by the ImageJ software using a grey scale mode. Moreover, the standard addition method was used to determine the concentration of cysteine in urine samples. The human urine samples used in this research were obtained from Environmental Analysis Research Unit (EARU) members.

.1.4 The benefit of this research

A new method for clinical screening of cysteine level in urine samples was obtained.

CHAPTER II

THEORY

2.1 Hydroxyapatite

Hydroxyapatite (HAp) has a formula of $Ca_{10}(PO_4)_6(H_2O)_2$ with atomic Ca/P molar ratio of 1.67. Because of the similar chemical composition with the component of natural bone, HAps are widely used in calcified hard tissue e.g. in orthopaedic as an implant to repair, fill, extend or reconstruct the damaged bone tissue and in dental reconstruction. It also used as a coating on materials such as a coating on titanium and titanium alloys as bioactive properties such as knee joint replacements [21, 22, 25].

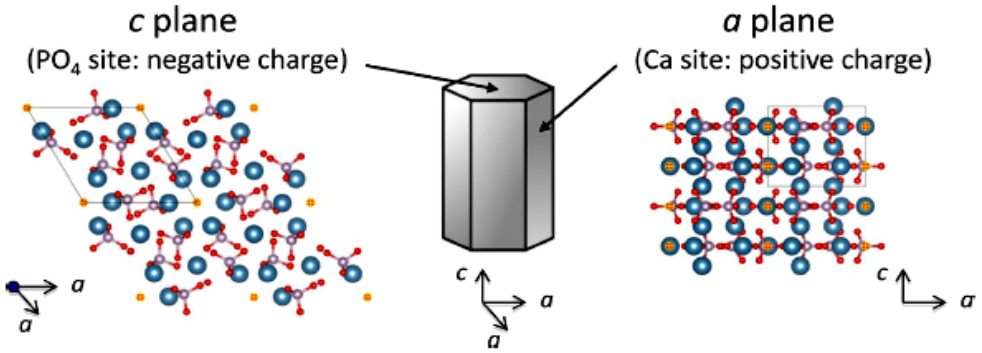

Figure 2.1 Crystal plane of hydroxyapatite. Plane A is rich in Ca^{2+} ions charge while plane B is rich in phosphate and hydroxide ions [24]

2.1.1 Properties of hydroxyapatite

HAps are stable at room temperature and pH between 4-12. It has hexagonal crystalline structure with two major crystal planes, ***a*** plane as positively charged plane rich in calcium ions, and ***c*** plane as negatively charged plane rich in phosphate and hydroxide ions as seen in Figure 2.1 [24]. Because HAp contains both cations and anions in its structure, it has high affinity for organic molecules. Moreover, Ca^{2+} ions on HAp can be replaced with other cations such as Ag^{+}, Mg^{2+}, Na^{+}, and K^{+} causing a slight change in the *a* and *c* lattice parameters compared to the original HAp [24, 26]. Because of this cation replacement, hydroxyapatite is widely used for removal of heavy metal ions such as Cd^{2+} [27], Pb^{2+} [28], Cr^{3+}, Zn^{2+} [29], and Cu^{2+} [30] in an aqueous solution.

Besides substitution of cations, anions on HAps can also be substituted with other anions as follows: F^{-} and Cl^{-} substitute OH^{-} while CO_3^{2-} and SiO_4^{4-} substitute PO_4^{3-} on HAps. Moreover, HAp has high tolerance for ion substitution, where OH^{-}, PO_4^{3-} and Ca^{2+} ions can be substituted without changing the structure [31].

2.1.2 Synthesis of Hydroxyapatite

The methods of HAp synthesis are classified into wet chemistry methods and solid-state reactions. The wet chemistry methods include precipitation method, sol–gel method, hydrothermal reactions, and emulsion and micro-emulsion method,

while solid state reactions typically are the reactions between β-tricalcium phosphate (TCP) and $Ca(OH)_2$ powders [32-37].

$$10\ Ca^{2+} + 6\ PO_4^{3-} + 2OH^- \longrightarrow Ca_{10}(PO_4)_6(OH)_2 \quad (2.1)$$

The precipitation method is the most commonly used method using an aqueous solution of calcium and phosphate in a basic solution (Eq. 2.1). This method is simple and inexpensive, requires few numbers of chemicals, produces HAPs nanoparticles and gives only water as by-product. The reaction is performed at temperature between 25 and 90°C. Adjusting the mixture pH to a value of 9 or higher during the process can increase the production rate of hydroxyapatite. A solution of ammonium hydroxide is generally used to adjust the pH of solution. Furthermore, washing the obtained crystal is necessary to remove residual nitrate and ammonium hydroxide [21, 22, 38].

2.1.3 Modification of hydroxyapatite with Ag^+

Hydroxyapatite can be modified with specific cations to improve its properties to suit its applications. Examples of several cations substituted on Haps and its specific applications are as follows: Co^{2+} modified on HAp giving catalytic effect for specific reactions [39] and Ag^+ gave antibacterial effect of HAp [40].

Insertion of Ag^+ into the HAp structure could be achieved by several approaches. Silver ions could be introduced into crystal structure either by doping

them during the co-precipitation reaction [26, 35] or through ion exchange or diffusion mechanisms [26, 40]. In the doping of Ag^{+} on HAp by co-precipitation method, Ag^{+} is added in the starting mixture at a (Ca+Ag)/P ratio of 1.67. On the other hand, in the doping of HAp with Ag^{+} via ion exchange method, silver ions solution is added onto HAp solid. Santos *et al.* [26] compared the preparation of Ag^{+} modified Hap by the co-precipitation and diffusion method. In the diffusion method, Ag^{+} replaced some of Ca^{2+} ions on the surface via ion exchange mechanism. Ag^{+} could substitute Ca^{2+} on HAPs through interaction with phosphate on HAp and the resulting agglomerates size was different from that of the original HAp. Moreover, the insertion Ag^{+} into HAp structure caused changes in *a* and *c* lattice parameter compared to the original HAp after 1h of the synthesis.

2.2 Silver nanoparticles

Silver nanoparticles (AgNPs) are the most widely used material in nanotechnology products because of its physical and chemical properties including high electrical and thermal conductivity, surface-enhanced raman scattering, chemical stability, catalytic activity, and non-linear optical properties. The size, shape, environment, chemical composition and surface chemistry of the silver nanomaterial determine its physical, chemical, and optical properties [41].

As mentioned before, the size of AgNPs is one of determinants of optical properties which relate to surface plasmons resonances. Surface plasmons are collective excitation of electrons resulted from interaction between electromagnetic wave with AgNPs described by evanescent electromagnetic waves (Figure 2.2). The characterization of collective oscillations of the electron cloud are determined by a surface charge distribution whilst frequency of each collective oscillation of electron cloud is determined by the electron density, effective mass, and the shape of the particle [42, 43].

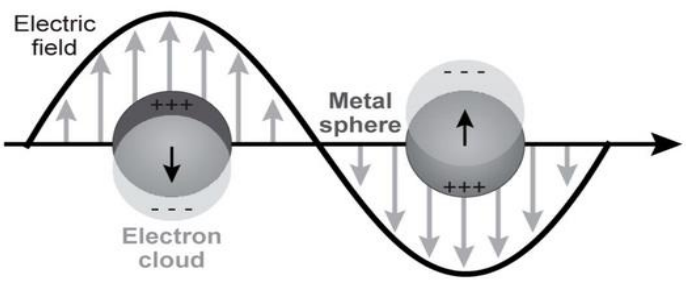

Figure 2.2 Illustration of the localized surface plasmon resonance [43]

Exhibiting broad spectrum of anti-bactericidal and anti-fungicidal properties, AgNPs have been applied in surgical, food handling, packaging and storage tools, water purifiers, textiles, cosmetics, contact lens cases, wound care products, implantable devices, and more recently drug delivery [41, 44]. The using of AgNPs as anti-bactericidal and anti-fungicidal is because the majority of cell materials and also DNA of bacteria and other microbes are made from sulphur and phosphorus which are soft

base while AgNPs is soft acid. Because interaction between AgNPs and sulphur causes cell damage, therefore it leads to the cell death [44].

2.3 Cysteine

Cysteine, a thiol-containing non-essential amino acid, has important roles in protein synthesis, detoxification, and diverse metabolic functions. As a strong antioxidant, thiol group acts as nucleophilic undergoing addition and substitution reaction. It also has high binding affinity toward heavy metals. For biochemical research, determination of the level of sulphur-containing compounds is important especially in the study of thiols drugs or the diagnosis of diseases such as cystinuria and homocystinuria [1, 3].

In human body, the sources of cysteine are from diets, methionine degradation, and proteins breakdown [3]. The concentration of total cysteine in biological fluid samples such as urine of healthy individuals is in the range of 20-200 μM [4-8, 10].

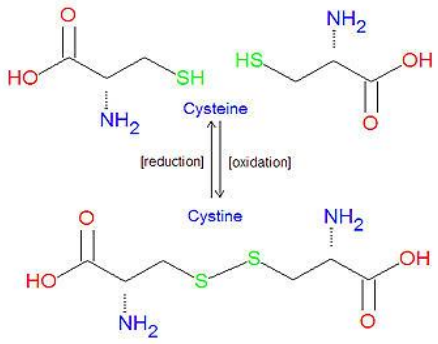

Figure 2.3 reversible oxidization-reduction system of cysteine-cystine

However, the presence of excessive amount of cysteine causes impaired resorption which could increase the possibility of cysteine oxidation to form cystine (Figure 2.3) and cause stone disease called cystinuria in kidney, bladder, or ureters. The solubility of cysteine stone or cystine in urine is approximately 250 mg/L (1mM/L) at pH up to 7 whilst at pH above 7, the solubility increases up to more than two times [9]. Consumption of large amount of fruits and vegetables especially citrus fruits can produce alkaline urine and help prevention of cysteine stone formation. Moreover, excessive loss of cysteine can also cause hereditary disorder [1, 3].

2.3.1 Determination cysteine by using nanoparticles

Nanoparticles such as silver nanoparticles (AgNPs) and gold nanoparticles (AuNPs) were applied to detect cysteine in rat brain [16], in an aqueous samples [17-19], and in biological fluids such as serum samples [20] and urine samples [7, 8]. Thiol group on the cysteine may interact with either AgNPs or AuNPs to form Ag–S or Au–S bond [17, 18]. The addition of salt solution such as NaCl in the system intends to reduce electrostatic repulsion between AuNP/cysteine or AgNP/cysteine in solution, thus induce the aggregation of nanoparticles [7, 17]. Then, the addition of other cations such as Ca^{2+} and Cu^{2+} would bind with amino ($-NH_2$) and carboxylate (-COOH) groups of cysteine on the nanoparticles resulting in chain-like aggregates of cysteine-coated AuNPs or AgNPs. Consequently, the color of solution changes depending on the concentration of cysteine as illustrated in Figure 2.4 [15, 17-20].

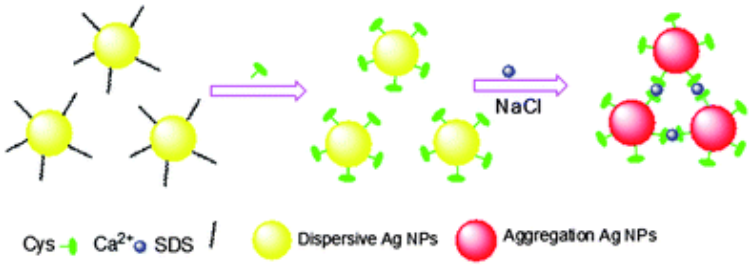

Figure 2.4 Schematic representation of the analytical process for detecting cysteine using AgNPs [20].

2.3.2 Sample collection, storage and preparation cysteine

Diet and lifestyle are determinants of the components containing urine. The normal urine usually does not contain proteins and lipids. Because cysteine can be easily oxidized to form cystine, the analysis of cysteine is conducted immediately after sample collection. Therefore, urine samples are collected randomly for the analysis of thiols [45]. Kusmierek *et al.* [45] reported that cysteine in urine sample was fairly stable in early hours after urine collection. Based on the result, the analysis of cysteine should be done within 4-5 h after sample collection.

Furthermore, to suppress the conversion of thiol to disulphide, addition of a chelating agent, alkylation of reduced thiol groups, and acidification of the samples can be performed. Chelating agent (*e.g.* ethylene diaminetetraacetic, EDTA) can form complex with metal ions such as Fe^{3+} [46] that act as non-enzymatic catalyst of thiol group oxidation. The alkylation reagents should be susceptible to nucleophilic attack

by the cysteine sulphur. Iodoacetic acid is an example of the reagent which prevents the formation of oxidized cysteine by deactivated thiol group on cysteine [47, 48]. On the other hand, acidification of samples suppresses the oxidation of thiol group on cysteine by protonating all functional groups on cysteine (Figure 2.5). However, acidification of the sample is often not suitable for reduction, derivatization, or pre-treatment steps in further analysis.

Figure 2.5 pKa values of cysteine and its deprotonated forms

2.4 Cation Exchange Resin

Ion exchange resin is polymer resin containing positively or negatively charged groups and its counter ions that can be exchanged with ions of the same charge. The ions are attached to the charged groups on the resin via electrostatic attraction. Ion exchange resins are widely used in separation, purification, and decontamination processes.

Strong cation exchange resins (CER) contain strong acid functional groups such as sulphonic acid ($–SO_3H$) as shown in Figure 2.6 that can be deprotonated to sulfonate groups as cation exchanger with negative charge. The counter ions such as proton can

be exchanged with other cations in solution. The cations affinity against to CER is determined by ionic size and charge of the cation. Moreover, the affinity order of some common cations in dilute solutions [49] is as follows.

$$Hg^{2+} < Li^{+} < H^{+} < Na^{+} < K^{+} \approx NH_4^{+} < Cd^{2+} < Cs^{+} < Ag^{+} < Mn^{2+} < Mg^{2+} < Zn^{2+} < Cu^{2+} < Ni^{2+} < Co^{2+} < Ca^{2+} < Sr^{2+} < Pb^{2+} < Al^{3+} < Fe^{3+}$$

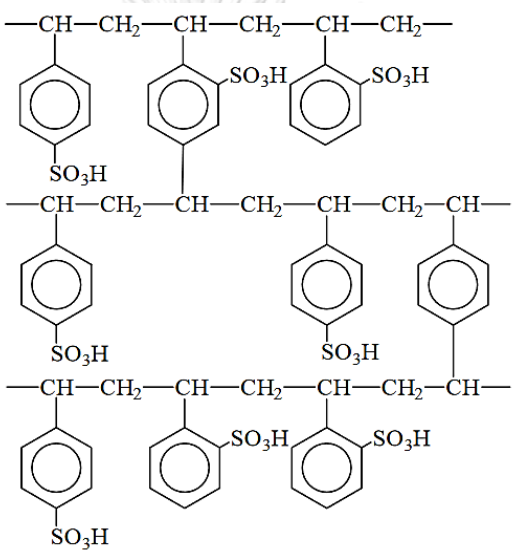

Figure 2.6 A strongly acidic sulfonated polystyrene cation exchange resin [49]

CHAPTER III

EXPERIMENTAL

3.1 Chemicals

The chemicals solutions used in this research was prepared in deionized water. The chemicals listed in table 3.1 were analytical grade.

Table 3.1 The list of chemicals used in this work

Chemicals	Supplier	Purity
Ammonia solution	Merck	25 %
Calcium nitrate ($Ca(NO_3)_2$)	RPE	99-103 %
Cation Exchange Resin	Dowex	-
Cysteine	Sigma-Aldrich	97 %
Cystine	Sigma-Aldrich	-
Homocysteine	Sigma-Aldrich	≥ 95 %
Methionine	Sigma-Aldrich	98 %
Nitric acid	Merck	65 %
Phosphoric acid (H_3PO_4)	RPE	85 %
Silver nitrate ($AgNO_3$)	AEN CORE	99.9 %
Sodium borohydride ($NaBH_4$)	Lobal Chemie	97 %
Sodium hydroxide	Merck	99.9 %

3.2 Preparation and characterization of hydroxyapatite

3.2.1 Synthesis of hydroxyapatite powder

Hydroxyapatite was synthesized via a precipitation method by mixing H_3PO_4 and $Ca(NO_3)_2$ solutions (Eq. 3.1). To get 20 mg of HAp, 47.013 g of $Ca(NO_3)_2.4H_2O$ were dissolved in 50 mL of DI water whilst 6.83 ml of H_3PO_4 were diluted into 25 mL of DI water. These amounts give a Ca/P-mole ratio of 1.67 for forming HAp. The diluted H_3PO_4 solution was then added dropwise into the $Ca(NO_3)_2$ solution. The pH of solution was then adjusted to 10 by adding an ammonia solution and kept at this pH during the mixing process for 1.5 h. The obtained mixture was centrifuged, and the solid was washed with deionized water to remove the excess amount of ammonia and dried at 120^0C overnight in an oven.

$$10\ Ca(NO_3)_2 + 6H_3PO_4 + 20\ NH_4OH \longrightarrow Ca_{10}(PO_4)_6(OH)_2 + 20\ NH_4NO_3 + 18\ H_2O \quad (3.1).$$

3.2.2 Characterization of prepared hydroxyapatite

The crystalline phases of the synthesized hydroxyapatite powders were identified by X-ray diffraction (XRD) using Rigaku, D/max-2200 Ultima + diffractometer equipped with a monochromator and a Cu anode operated Kα radiation source. The 2θ angle of the X-Ray beam was in the range of 20^0 to 55^0 degrees during screening. Moreover, the morphology of the materials including size and shape of HAp, AgNPs

containing HAp was examined by using transmission electron microscopy (TEM), JEM-2100 from JEOL.

3.3 Preparation of silver hydroxyapatite nanoparticles

Hydroxyapatite was modified with Ag^+ via doping by ion-exchange (Eq. 3.2). A $AgNO_3$ solution (16 mg/L, 1.00 mL) was added onto HAp (40 mg) and stirred for 2 min. The mixture was centrifuged to separate the solid from the solution.

$$Ca_{10}(PO_4)_6(OH)_2 + Ag^+ \longrightarrow Ca_{(10-n)}Ag_n(PO_4)_6(OH)_2 \qquad (3.2)$$

Some parameters including the reaction time between Ag^+ solution and HAp and the concentration of Ag^+ were studied.

3.4 Detection cysteine in standard solution and synthetic urine

Detection of cysteine of different concentrations in standard solutions (0-50 μM) was investigated. 2.8 mL of cysteine sample solution was added onto the Ag^+ modified-HAp and stirred for 2 min. After discarding the solution, 30 μL of 10 mM $NaBH_4$ was added and mixed for 2 min. The solid was filtered onto a filter paper for onsite color observation. The photo of the solid was taken in a black box and subjected to Image-J program to measure the color intensity. The effect of $NaBH_4$ volume was investigated to ensure a total reduction of Ag^+ to AgNPs.

In order to investigate the effect of matrix on the analysis, cysteine in synthetic urine solutions was prepared and used in the experiment. The composition of synthetic urine and their levels are listed in the Table 3.2 [50]. These chemicals were dissolved in deionized water and mixed together.

Table 3.2 Composition of synthetic urine

No	Chemical	Formula	Mass (mg) in 100 mL of DI	Concentration (mg/L or ppm)
1	Ammonium chloride	NH_4Cl	100	1000
2	Calcium chloride	$CaCl_2$	56	560
3	Creatinine	$C_4H_7N_3O$	110	1100
4	Magnesium chloride	$MgCl_2$	31	310
5	Potassium chloride	KCl	160	1600
6	Potassium dihydrogen phosphate	KH_2PO_4	280	2800
7	Sodium chloride	NaCl	460	4600
8	Sodium sulphate	Na_2SO_4	230	2300
9	Sodium oxalate powder	$Na_2C_2O_4$	2	20
10	Trisodium citrate	$Na_3C_6H_5O_7$	65	650
11	Urea	CH_4N_2O	2,500	25,000

3.5 Activation of cation exchange resin

Cation exchange resin was activated by diluted nitric acid. The resin and acid solution were mixed with the ratio 1:2 (mass : volume). The mixture was stirred overnight and washed with deionized water until the pH of runoff was neutral.

3.6 Sample pre-treatment and cysteine detection

Sample pre-treatment consisted of two steps, extraction and elution step. The sample pre-treatment was schematically presented in Figure 3.1. Prior to the extraction step using cation exchange resin (CER), sample pH was adjusted to pH 2 or lower to convert cysteine to its protonated form. 300 µL of 4 M HNO_3 was added into 32.00 mL of sample and the mixture was then mixed with 1.6 mL of cation exchange resin for 5 min. CER was then separated and washed with DI water.

In the elution step, the mixture solution of 600 µM of 2 M NaOH and 9.00 mL of the solution of 2 mM $Ca(NO_3)_2$ was added to the obtained CER and stirred for 5 min to elute the extracted cysteine. The eluted sample solution was collected and further analysed using Ag^+ modified HAp for cysteine detection. In the sample pre-treatment step, the effect of extraction and elution time, the NaOH addition, the concentration of Ca^{2+}, and volume of eluent sample were studied. In this work, each urine sample was diluted five-fold to minimize interferences effect. The diluted sample was further undergone sample pre-treatment as previously described.

Sample pre-treatment step:

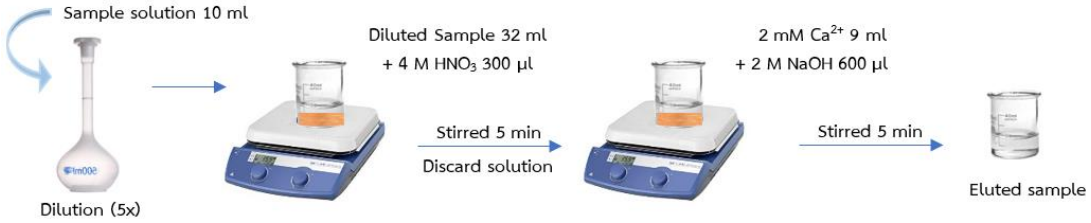

Detection step:

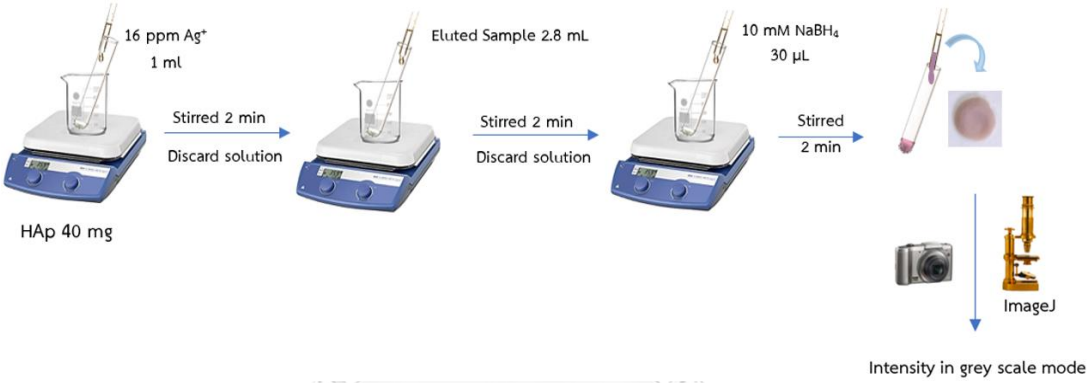

Figure 3.1 The procedures of sample preparation and cysteine detection.

3.7 Selectivity test

Before applying this proposed method to urine sample analysis, the selectivity of this method toward cysteine detection was evaluated in standard solutions in either the absence or the presence of another sulphur–containing amino acids such as methionine, cysteine or homocysteine. The color of AgNPs-HAps obtained was compared. The concentrations of cysteine used were 30 µM and 60 µM, while the chosen concentration of other sulphur–containing amino acids was based on its

concentration found in human urine sample (20 μM cystine, 8 μM methionine, and 10 μM homocysteine) [4-8, 10]. One-way ANOVA was then used to evaluate the effect of another sulphur–containing amino acids presence in the analysis with 95% confidence level and α = 0.05.

3.8 Method Performance

The performance of the proposed method was evaluated under the optimal condition. The method was applied to human urine sample analysis. Linear range, accuracy and precision were determined.

3.8.1 Linearity and working range

First, the linear range of the determination was determined using cysteine standard solutions. Then standard addition method was applied to determine concentration of cysteine in the urine samples. The calibration curve of standard addition method was established under optimal condition obtained before. The calibration curve was constructed using delta color intensity (the difference between color intensity of blank and sample) as y axis and concentration of added cysteine in the range of 0 – 60 μM as x-axis. The linearity of this method was then reported in terms of correlation coefficient value (R^2).

3.8.2 Accuracy and precision

The accuracy of this method was evaluated by determining percentage of recovery by spiking the known amount of cysteine into the sample with particular level concentration. In this present work, the concentrations of spiking were 15, 20, and 24.9 μM. Percent recovery can be calculated using Equation 3.3. Based on the AOAC International [51], percent recovery of the spiked analyte should be in the range 80-110 to be accepted as shown in Table 3.3.

$$\text{Recovery (\%)} = \frac{\boldsymbol{found\ cysteine}}{\boldsymbol{added\ cysteine}} \times 100\ \% \qquad (3.3)$$

The precision of this method was presented in terms of percentage of relative standard deviation (% RSD) value which should not be higher than 7.3 (Table 3.3) as based on the AOAC International [51].

Table 3.3 Percent recovery and percent RSD in the presence of different analyte concentration according to AOAC international

Analyte (%)	Mass fraction	Unit	Recovery range (%)	RSD (%)
100	1	100%	98-102	1.3
10	10^{-1}	10%	98-102	1.9
1	10^{-2}	1%	97-103	2.7
0.1	10^{-3}	0.1%	95-105	3.7
0.01	10^{-4}	100 ppm	90-107	5.3
0.001	10^{-5}	10 ppm	80-110	7.3

0.0001	10^{-6}	1 ppm	80-110	11
0.00001	10^{-7}	100 ppb	80-110	15
0.000001	10^{-8}	10 ppb	60-115	21
0.0000001	10^{-9}	1 ppb	40-120	30

3.9 Detection of cysteine in urine sample

The urine samples were collected from healthy adult volunteers from Environmental Analysis Research Unit (EARU) members, and the analysis was conducted immediately after sample collection. The standard addition method was used to determine concentrations of cysteine in urine samples. A stock solution of cysteine was prepared in deionized water and diluted to obtain working solutions in the range of 0 – 60 μM. 50 μL of working solution was then added in to the 9.95 mL of urine sample to obtain the concentration in a range of 0 to 60 μM. These spiked samples were diluted five-fold to decrease the interferences effect, and it was then undergone the pre-treatment step prior to the detection step as previously described. The color intensity of the solid obtained after the analysis of every samples was observed by naked eyes and measured by the ImageJ software using grey scale mode. The results were used to construct a calibration curve of the standard addition method and the concentration of cysteine in the urine sample was determined.

CHAPTER IV
RESULTS AND DISCUSSION

The main idea of this work is to determine the amount of cysteine based on the aggregation of silver nanoparticles on hydroxyapatite induced by cysteine. Hydroxyapatite was synthesized and further modified with silver ions (Ag-HAp) for the use in the detection of cysteine. Due to the matrix interferences on the analysis, sample preparation was applied in this work by using cation exchange resin to extract cysteine from urine sample.

4.1 Characterization of hydroxyapatite and silver-hydroxyapatite

The crystalline structure and phase purity of the synthesized HAp were confirmed by X-ray diffraction (XRD) in the 2θ range from 20^0 to 55^0. The XRD pattern of the crystal was compared with the standard database (JCPDS card 9-0432) as shown in Figure 4.1. The XRD pattern of the prepared material corresponded to hexagonal structure and in agreement with the standard pattern.

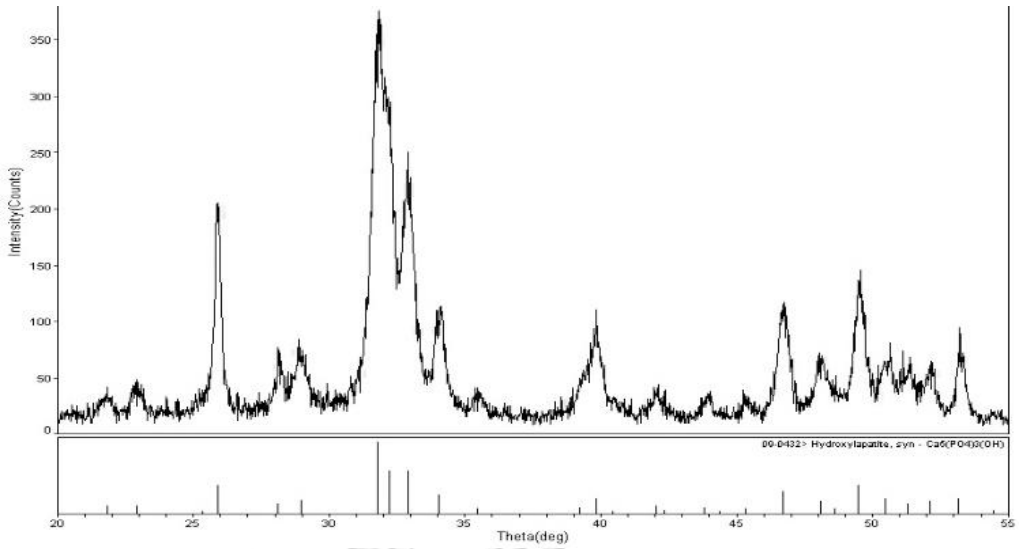

Figure 4.1 XRD pattern of the prepared hydroxyapatite.

The morphology of the materials was observed using a transmission electron microscope (TEM). The prepared hydroxyapatite (Figure 4.2 A) had rod-like and needle like shape with the particle size around 60-70 nm. Moreover, the successful modification of HAp with Ag^{+} via extraction was confirmed by the presence of the spherical particles of AgNPs on the HAp after adding a $NaBH_4$ solution as shown in Figure 4.2 B.

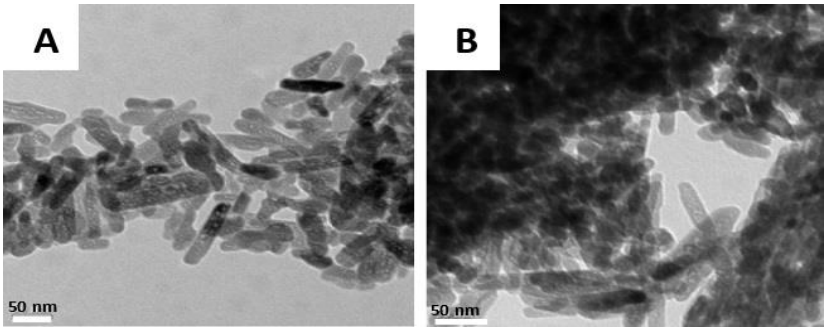

Figure 4.2 TEM images of Hydroxyapatite, HAp (A) and hydroxyapatite in the presence of silver nanoparticle, AgNPs-HAp (B).

4.2 Silver-hydroxyapatite nanoparticles preparation

The silver ions-modified hydroxyapatite (Ag-HAp) was prepared by extracting Ag^+ onto HAp via doping ion-exchange. Ag^+ substitutes Ca^{2+} on the HAp through ion exchange mechanism. Extraction of Ag^+ on HAPs can also occur via interaction with a phosphate ion on HAps [26]. The presence of Ag^+ on HAp was observed by adding $NaBH_4$ to reduce Ag^+ onto HAp to AgNPs. The AgNPs formed were observed by TEM as spherical particles on HAp (Figure 4.2 B), and the color of HAp turned to yellow. Moreover, some influence parameters such as Ag^+ concentration, reaction time between a Ag^+ solution and HAp were optimized.

4.2.1 Effect of Ag^+ concentration

The concentration of Ag^+ used to modify HAp was varied to get a sufficient amount of silver on HAp for the further detection of cysteine. The concentration of Ag^+ was selected based on the highest concentration of cysteine possibly found in samples. The modified materials were used to detect 30 μM cysteine and the results are shown in Table 4.1.

Table 4.1 Color on HAp observed at the different concentrations of Ag^+ after adding $NaBH_4$

cysteine (μM)	Ag^+ (mg/L)		
	16	12	8
0			
30			

An increase in Ag^+ concentration from 8 to 16 mg/L resulted in more intense color of AgNPs on HAp. At low concentration of Ag^+, a pale pink color on HAp was observed in the presence of cysteine indicating that the amount of Ag^+ on HAp was not sufficient to interact with cysteine. Using a solution containing 16 mg/L Ag^+ resulted in the most intense color of AgNPs on HAp. When the Ag^+ concentration was higher than 16 mg/L, the color of HAps in the absence of cysteine was dark yellow due to an excessive amount of Ag^+ which was not good for color change observation in the detection of cysteine at low concentrations. Therefore, the concentration of 16 mg/L was adopted for further study.

4.2.2 Effect of contact time between Ag^+ and HAp

The effect of interaction time between Ag^+ (16mg/L) and HAp for HAp modification was observed at 2, 4, 8, and 60 min. The amount of Ag^+ extracted was determined using inductively coupled plasma atomic emission spectroscopy (ICP/AES). As shown in Figure 4.4, the HAp could extract 81 % of Ag^+ from solution within 2 min. Prolonging the time period to longer than 2 minutes did not remarkably increase the amount of Ag^+ on HAp. Therefore, the extraction time of 2 min was selected.

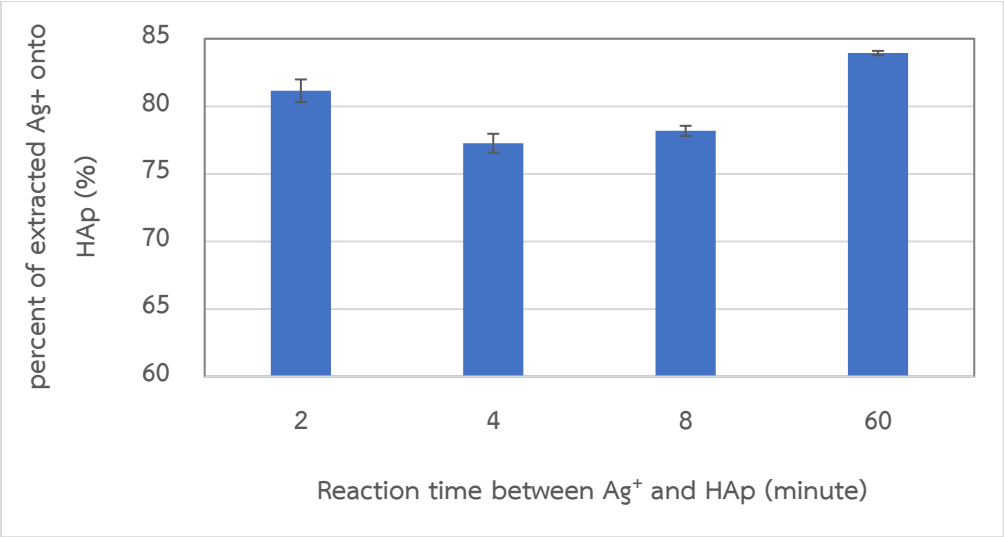

Figure 4.3 Effect of contact time on the efficiency of Ag^+ extraction on HAp.

4.3 Detection of cysteine in standard solutions

HAp modified by Ag^+ (Ag-HAp) was then used as the material to detect cysteine in standard solutions. The presence of cysteine with adding $NaBH_4$ induced the aggregation of AgNPs to form larger AgNPs clusters on HAp, and the color of solid containing AgNPs changed from yellow in the absence of cysteine to yellow-pink and violet in the presence of low and high concentrations of cysteine, respectively. The color change could be observed by naked eyes and the color intensity was measured by the Image J program. The AgNPs on HAp was observed by TEM (Figures 4.4A and B). TEM images reveal that the cluster size of AgNPs was larger in the presence of cysteine of higher concentration.

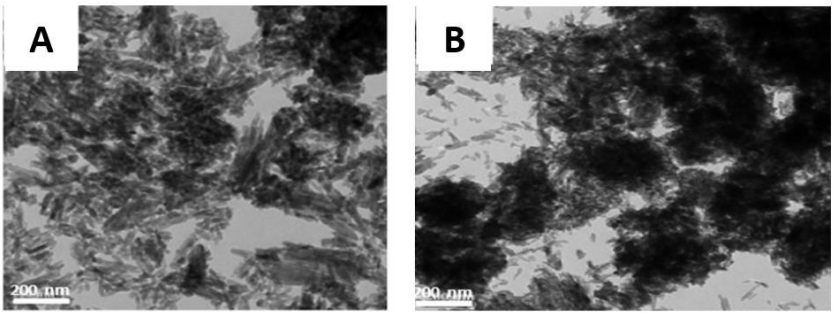

Figure 4.4 TEM images of AgNPs-HAp in the presence of 5μM cysteine (A), and AgNPs-HAp in the presence of 30 μM cysteine (B).

The mechanism of the cysteine detection using HAp modified with Ag^+ is illustrated in Figure 4.5. The reaction between cysteine and Ag^+ on HAp occurs through interaction with thiol group which has strong affinity toward metal ions. Besides that, cysteine as zwitterion exists in a partly ionized form containing electron-donor groups ($-NH_2$) and –COOH) that enable it to coordinate with Ag^+ [52]. When $NaBH_4$ solution is added, Ag^+ is converted into AgNPs and the presence of cysteine induces the formation of AgNPs clusters on HAp.

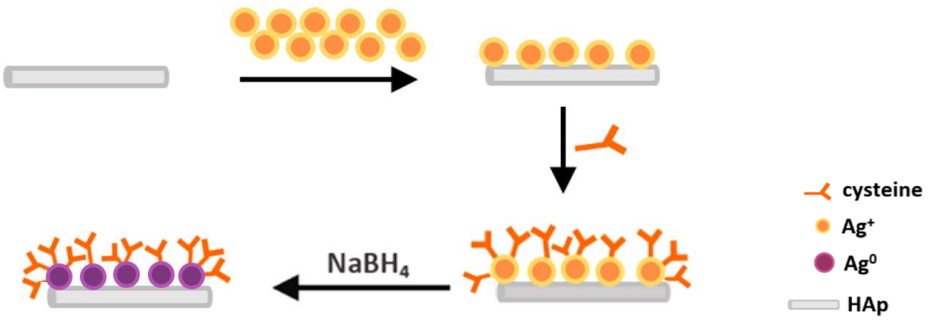

Figure 4.5 Schematic illustration of the mechanism of cysteine detection.

4.3.1 Effect of $NaBH_4$ volume

The volume of 10 mM $NaBH_4$ solution was varied to confirm whether it has any effect on the analysis and to ensure a total reduction of Ag^+ to AgNPs observed by change color. Table 4.2 shows that increasing volume of $NaBH_4$ resulted in more yellowish shade on HAp in the presence of same concentration of cysteine. On the other hand, at the lowest added volume of $NaBH_4$ solution (30 µL), the color of HAp was pink violet. This result could be explained that the reduction of Ag^+ under lower content of $NaBH_4$ may occur more slowly and the aggregation could take place better, resulting in a bigger size of AgNPs cluster shown as pink violet color on HAp. Therefore, the volume of 30 µL was chosen for the further experiments.

Table 4.2 Color of AgNPs-HAp obtained by using different volumes of $NaBH_4$ solution

cysteine (µM)	Volume of $NaBH_4$ 10 mM (µL)						
	30	60	100	200	300	400	600
0							
30							

4.3.2 Effect of sample matrix

Based on the results obtained previously, the method was then applied to detect cysteine of different concentrations in standard solutions and in synthetic urine to observe the interferences effect. The results are shown in Table 4.3. The concentration of cysteine ranged from 0 to 50 µM was adopted as working

concentration range. The results show that the color of AgNPs-HAp changed from yellow to pink and violet in increasing cysteine concentration in standards solutions. On the other hand, the color of AgNPs-HAp used to detect different concentrations of cysteine in synthetic urine was not distinguishable at a concentration range of 0 to 30 μM. It proved that the matrix of synthetic urine seemed to prevent the aggregation and had influence on the analysis. Furthermore, the color intensity of the solids was measured by Image J software in grey scale. A calibration curve was constructed by plotting delta color intensity (ΔI) which is the difference between the intensity of blank and the standard solution, as *y*-axis and the concentration of cysteine in the range of 0 to 50 μM as *x*-axis (Figure 4.6).

Table 4.3 Color of AgNPs-HAps obtained in the detection of different concentrations of cysteine in standard solution and in synthetic urine

Matrix	Concentration of cysteine (μM)					
	0	10	20	30	40	50
Deionized water						
Synthetic Urine						

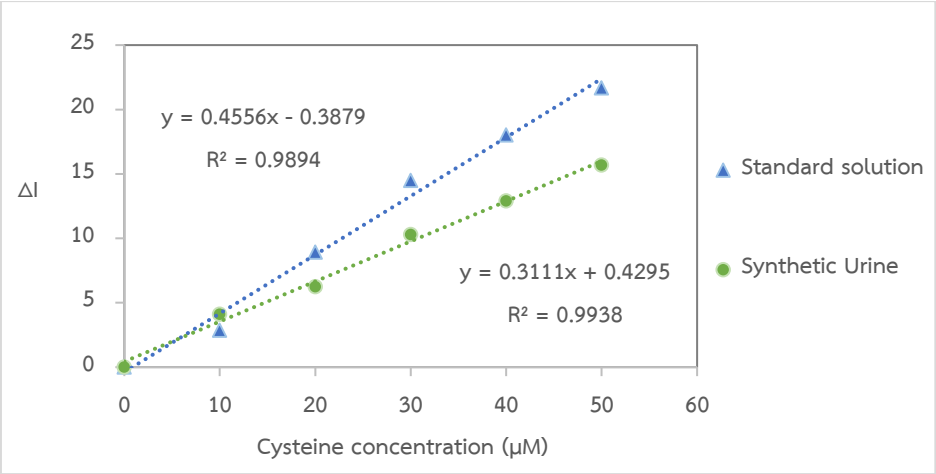

Figure 4.6 Calibration curve of cysteine detection in standard solutions and in synthetic urine.

The linear relationship was obtained in this concentration range. However, the results clearly show that the detection of cysteine in urinary matrix was much less sensitive than that in the standard solution as shown as the lower slope. It is likely that the interferences such as Cl^- in synthetic urine competitively interacted with Ag^+ on HAps, thus there was less number of Ag^+ available for binding with cysteine. Therefore, sample preparation is required in the detection of cysteine in urine sample.

4.4 Sample preparation and detection of cysteine

Sample preparation was required for diminishing the interferences effect in the analysis. By adjusting sample pH to be lower than 2, all functional groups on cysteine was protonated ($-NH_3^+$, -COOH), and carry a positively charged (Figure 2.5). Cation

exchange resin (CER) was then used for extracting cysteine from the sample (Figure 4.7). A solution of Ca^{2+} was then used to elute cysteine from the resin through ion exchange mechanism. Ca^{2+} was selected to replace the protonated cysteine containing NH_3^+ group because it has higher affinity toward sulfonate groups on the cation exchange resin than the ammonium group ($-NH_3^+$) [49].

The addition of NaOH with the certain amount in the Ca^{2+} solution is expected to increase the efficiency of cysteine elution from CER by deprotonating all functional groups on cysteine. Furthermore, it also neutralizes the eluted sample before the detection step. However, an excessive amount of NaOH would cause silver hydroxide precipitation on HAp and reduce the content of Ag^+ ions on HAps.

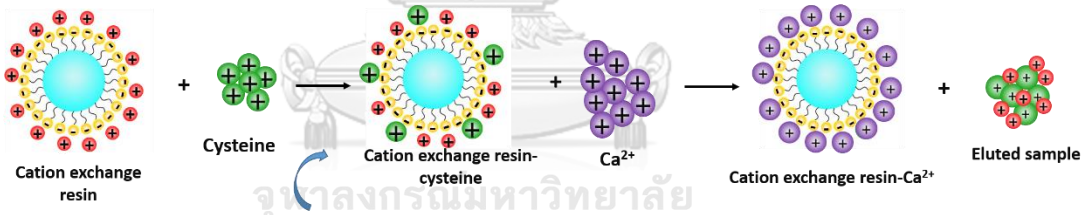

Figure 4.7 Sample preparation step

The effect of several influence parameters in sample preparation such as the concentration of Ca^{2+}, NaOH addition, and extraction and elution time were studied using cysteine standard solutions.

4.4.1 The effect of eluent concentration

Eluents containing varied concentration of Ca^{2+} (1, 2, 4, 6 mM) were used in the sample preparation and the results are shown in Table 4.4. Ca^{2+} was expected to replace the extracted cysteine on CER, and hence, the aggregation of AgNPs induced by a quantitative amount of eluted cysteine would be obtained. It was observed that HAp has more intense pink color in increasing the concentration of Ca^{2+} from 1 mM to 2 mM.

The concentration of Ca^{2+} at 1 mM was not enough to elute cysteine from CER. However, at concentration higher than 2 mM, disaggregation of AgNPs on HAps occurred as the paler pink shade to yellowish shade of HAps color was observed. It was probably triggered by the enhanced surface charge due to an excessive amount of Ca^{2+} on AgNPs surface. As a result, the AgNPs would repulse each other and aggregation did not occur.

Table 4.4 Effect of concentration of Ca^{2+} on the color of AgNPs-HAp

Concentration of cysteine (μM)	Concentration of Ca^{2+} (mM)			
	1	2	4	6
0	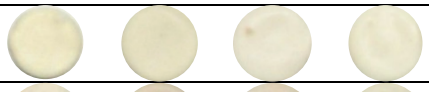			
40				

4.4.2 The effect of NaOH addition into eluent

Addition of NaOH in a Ca^{2+} solution also enhances the release of cysteine from CER by deprotonating all functional groups on cysteine. It was achieved by using 2 mM Ca^{2+} solution containing 0.125 M NaOH to elute cysteine on the CER after an extraction process. Table 4.5 shows that the distinguishable color of AgNPs-HAps used in the detection of different concentrations of cysteine (0 – 105 μM) was obtained by adding NaOH. Moreover, the addition of NaOH also increased the sensitivity of the analysis confirmed by the higher slope of the linear calibration curve from the linear regression (Figure 4.8). Therefore, the eluent containing 0.125 M NaOH was used in the further experiments.

Table 4.5 The effect of NaOH addition into 0.2 mM Ca^{2+} eluent on AgNPs-HAp color

Eluent	Concentration of cysteine (μM)							
Without NaOH	0	15	30	45	60	75	90	120
								
With NaOH	0	15	30	45	60	75	90	105
								

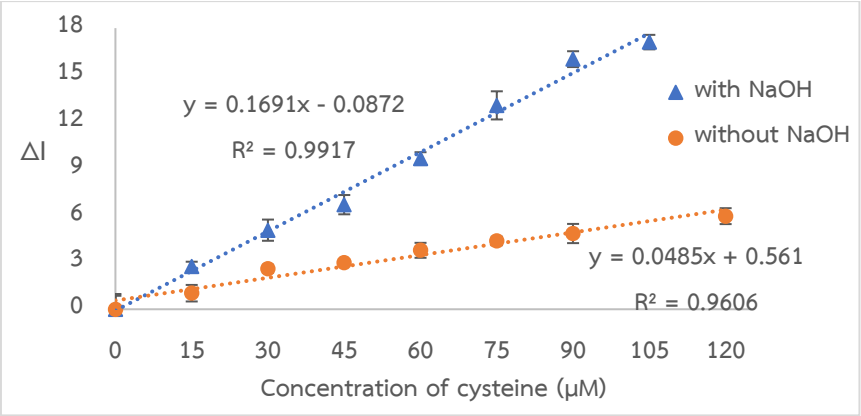

Figure 4.8 Calibration curve of cysteine detection in standard solution with sample preparation using eluent with and without 0.125 M NaOH.

4.4.3 Effect of extraction time and elution time

Before extraction and elution process, sample was diluted 5-fold for diminishing interferences in sample. The time for extraction and elution of cysteine was varied to get quantitative amount of cysteine for detection. The results are shown in Table 4.6.

Based on the observation of color by eyes, there was no distinguishable difference in color of AgNPs-HAps either using the extraction of 5, 8 and 10 min or using elution time of 5, 8, and 10 min. These results had been confirmed by statistical calculation using one-way ANOVA showing that there was no significant difference in color intensities of the solids used in detection of 40 μM cysteine (P = 0.4131) or 100 μM cysteine (P = 0.816) at the 95% Confidence level α= 0.05).

Table 4.6 Color on HAp observed at the different time of extraction and elution (color intensity as grey values are given under each photo)

Extraction time (min)	Elution time (min)								
	5			8			10		
5									
	194.71	192.10	181.42	195.82	193.59	181.00	195.11	190.81	179.88
8									
	194.32	191.34	181.06	194.26	191.74	181.28	194.23	192.21	182.37
10									
	194.02	193.04	181.07	194.83	192.53	181.07	194.72	191.88	182.34
	0	40	100	0	40	100	0	40	100
	Concentration of cysteine, μM								

4.4.4 Effect of eluted sample volume in detection cysteine

The influence of eluted sample volume used to mix with Ag-HAp in the detection step was further studied. The objective is to get a quantitative amount of cysteine onto Ag-HAp that results in distinguishable color when different concentrations of cysteine are detected. The sample volume was varied in the range from 1.60 to 3.40 mL. The result showed that the sample volumes of 2.80 and 3.40 mL gave more distinct color change in the presence of different concentrations of cysteine as shown in Table 4.7. Since the use of 2.80 and 3.40 mL of sample gave similar color, 2.80 mL of eluted sample volume was used in the method.

Table 4.7 Color on HAp observed using different eluted sample volume in the detection step

Cysteine concentration (μM)	Volume of eluted sample (mL)			
	1.6	2.2	2.8	3.4
0				
30				
60				
105				

4.5 Selectivity test

Amino acids containing sulphur atom would either compete with cysteine on the extraction by CER or induce the aggregation of AgNPs. The effect of cystine, methionine and homocysteine, which are the amino acids possibly found in human urine, was investigated. The selectivity of the method was evaluated by comparing the color of AgNPs-HAps in the absence and the presence of these amino acids. The chosen concentration of other sulphur-containing amino acids was based on its normal concentration found in human urine samples [4-8, 10]. The results are shown in Table 4.8.

The results show that there was no difference in the observed color on AgNPs-HAp in the absence and in the presence of another amino acid. It was also confirmed

statistically by one-way ANOVA using color intensities with P = 0.152 (for cysteine 30 μM) and P = 0.137 (for cysteine 60 μM) at the 95% confidence level and α = 0.05.

Table 4.8 Color of AgNPs-HAp observed in selectivity test in the presence of different sulphur containing amino acids

[**Concentration of cysteine (μM)**	**Concentration of added amino acid (μM)**		
	cystine	methionine	homocysteine
	20	8	10
30			
60			

4.6 Method performance

The performance of the proposed method was evaluated under selected condition that was obtained previously. The working range of this method was determined using standard solutions of cysteine.

4.6.1 Linearity and working range

Under the optimum experimental conditions, a calibration curve was then plotted between delta intensity of color (y-axis) against the concentration of cysteine (x-axis). The color intensity of each solid was measured by the Image J program when the photo of the solid was converted to red, blue, green, and grey scale.

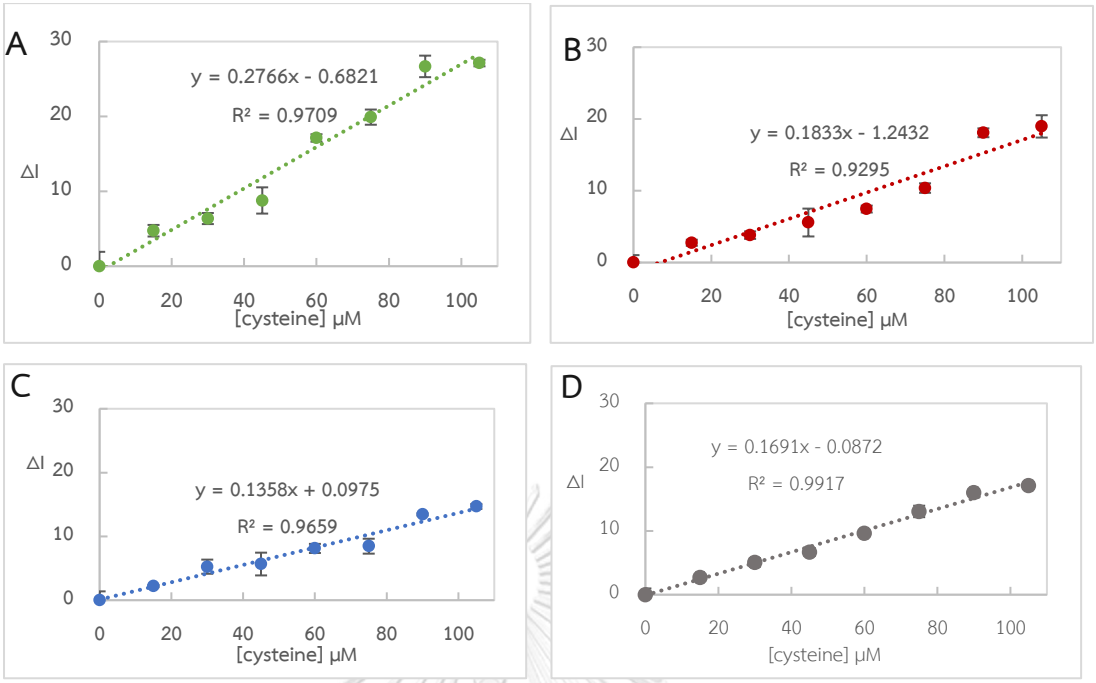

Figure 4.9 Calibration curve of cysteine in standard solution with sample preparation. Color intensity was measured in green (A), red (B), blue (C), and grey (D) scale mode.

From Figure 4.9, the linear relationship was obtained by using intensities in grey scale mode with a correlation coefficient of 0.9917 (Figure 4.5D), while the other color scales did not give the linear relationship. Using the grey scale mode, the working range of this method was in the range from 0 to 105 μM which covers the concentrations of cysteine found in urine sample [4-7]

4.7 Detection of cysteine in urine sample

The applicability and reliability of the current method was evaluated by applying the method to detect the level of cysteine in human urine samples. Pre-treatment of sample was required since matrix interference substances such as urea,

anions and cations from salts, other organic and inorganic compounds are usually present in the urine. The pre-treatment of sample consisted of the extraction on cation exchange resin (CER) and the elution step as described before. The condition in sample pre-treatment and detection obtained previously in this study was used.

However, the urinary matrix differs from person to person and hence the standard addition method was used to obtain the concentration of cysteine in real samples. To evaluate the accuracy of the method, the recovery of known amount of cysteine spiked to the urine sample was determined as shown in the Table 4.9. The proposed method gave percent recovery in the range of 92.0 to 111.9 %. The Urine I sample had percent recovery higher than 110 because of spiking a very low amount of cysteine (15 μM), thus color did not obviously change, and more error could occur in this case. In the other hand, the precision of this method was also evaluated and presented in terms of percentage of relative standard deviation (% RSD). This present method gave % RSD value in the range of 1.4-6.9 %. Moreover, percent recovery and percent RSD of the results are in an acceptable range in the criteria of AOAC International [51], indicating a good accuracy and precision of results obtained by this method.

Table 4.9 Determination of cysteine in urine sample

Sample	Cysteine concentration		Recovery (%)	RSD (%)
	Added (μM)	Found (μM)		
Urine I	0	10.8 ± 1.4	-	-
	15.0	27.5 ± 0.2	111.9 ± 1.6	1.4
Urine II	0	15.6 ± 0.5	-	-
	20.0	36.0 ± 0.6	102.3 ± 3.0	2.9
Urine III	0	15.8 ± 1.1	-	-
	20.0	35.9 ± 0.1	101.1 ± 3.0	3.2
Urine IV	0	10.2 ± 1.8	-	-
	20.0	29.5 ± 1.3	97.1 ± 6.9	6.9
Urine V	0	18.9 ± 4.0	-	-
	20.0	37.2 ± 0.90	92.0 ± 4.5	4.9
Urine VI	0	15.4 ± 3.7	-	-
	24.9	38.7 ± 0.7	93.7 ± 2.8	2.9

CHAPTER V
CONCLUSIONS

5.1 Conclusion

In the current study, the new method has been developed for detecting cysteine based on the aggregation of AgNPs on HAp in the presence of cysteine. The optimal condition for determination of cysteine was obtained by studying various parameters including extraction and elution time, concentration of Ca^{2+} solution, addition of NaOH, eluted sample volume, contact time between Ag^{+} and HAp, and concentration of Ag^{+}, and volume of $NaBH_4$ were studied to obtain optimal condition.

In order to overcome the matrix interfering effect, sample preparation, consisting of two steps; extraction and elution step, was required. Cation exchange resin (CER) was used to extract cysteine from the sample by adjusting sample pH to be lower than 2. A solution of Ca^{2+} containing NaOH was then used to elute extracted cysteine from the CER through ion exchange mechanism. The eluted cysteine the solution, as eluted sample, was then used in detection step.

The working range of this method using standard solutions was from 0 to 105 μM with a correlation coefficient, R^2, of 0.9917. The method is highly selective toward cysteine detection.

Due to the presence of various interferences levels in urine samples, the standard addition method was then used for the determination of cysteine in human urine. The accuracy and precision of this method were evaluated and presented in term of percent recovery and percent relative standard deviation (RSD), respectively. The results gave % recovery in the range of 92.0 to 111.9 along with % RSD in the range of 1.4 to 6.9 % which followed the AOAC International criteria.

5.2 Suggestion for future work

The using of reducing agent such as tris(2-carboxyethyl) phosphine, TCEP, may help to extend the reduced cysteine form during analysis, thus in determination of percent recovery may be done in 2 levels of concentration.

REFERENCES

1. Piste, P., *Cysteine–master antioxidant.* International Journal of Pharmaceutical, Chemical and Biological Sciences, 2013. **3**: p. 143-149.
2. Burns, A., P. Olszowy, and P. Ciborowski, *Biomolecules*, in *Proteomic Profiling and Analytical Chemistry: The Crossroads: Second Edition*. 2016, Elsevier Inc.
3. Yin, J., et al., *l-Cysteine metabolism and its nutritional implications.* Molecular nutrition & food research, 2016. **60**(1): p. 134-146.
4. Zhang, L., et al., *Determination of cysteine, homocysteine, cystine, and homocystine in biological fluids by HPLC using fluorosurfactant-capped gold nanoparticles as postcolumn colorimetric reagents.* Journal of separation science, 2014. **37**(1-2): p. 30-36.
5. Xiao, Q., et al., *Specific detection of cysteine and homocysteine in biological fluids by tuning the pH values of fluorosurfactant-stabilized gold colloidal solution.* Biosensors and Bioelectronics, 2011. **30**(1): p. 211-215.
6. Ševčíková, P. and Z. Glatz, *Specific determination of cysteine in human urine by capillary micellar electrokinetic chromatography.* Journal of separation science, 2003. **26**(8): p. 734-738.
7. Wei, X., et al., *A colorimetric sensor for determination of cysteine by carboxymethyl cellulose-functionalized gold nanoparticles.* Analytica chimica acta, 2010. **671**(1): p. 80-84.
8. Chen, S., et al., *Colorimetric detection of cysteine using noncrosslinking aggregation of fluorosurfactant-capped silver nanoparticles.* Sensors and Actuators B: Chemical, 2014. **190**: p. 673-678.
9. Biyani, C.S. and J.J. Cartledge, *Cystinuria—diagnosis and management.* eau-ebu update series, 2006. **4**(5): p. 175-183.
10. Bald, E., R. Glowacki, and J. Drzewoski, *Determination by liquid chromatography of free and total cysteine in human urine in the form of its S-quinolinium derivative.* Journal of Chromatography A, 2001. **913**(1): p. 319-329.

11. Głowacki, R., J. Stachniuk, and K. Borowczyk, *A simple HPLC—UV method for simultaneous determination of cysteine and cysteinylglycine in biological fluids.* Acta Chromatographica, 2016. **28**(3): p. 333-346.
12. Lim, S., et al., *Selective fluorescence detection of cysteine and N-terminal cysteine peptide residues.* Chemical Communications, 2010. **46**(31): p. 5707-5709.
13. Lee, P.T., et al., *Selective electrochemical determination of cysteine with a cyclotricatechylene modified carbon electrode.* Analyst, 2015. **140**(1): p. 236-242.
14. Lunar, M.L., et al., *Hexadecylpyridinium chloride micelles for the simultaneous kinetic determination of cysteine and cystine by their induction of the iodine-azide reaction.* Analytica chimica acta, 1997. **337**(3): p. 341-349.
15. Ivanov, A.V., et al., *Capillary electrophoresis coupled with 1, 1′-thiocarbonyldiimidazole derivatization for the rapid detection of total homocysteine and cysteine in human plasma.* Journal of Chromatography B, 2015. **1004**: p. 30-36.
16. Qian, Q., et al., *Aspartic acid-promoted highly selective and sensitive colorimetric sensing of cysteine in rat brain.* Analytical chemistry, 2012. **84**(21): p. 9579-9584.
17. Hajizadeh, S., et al., *Silver nanoparticles in the presence of Ca 2+ as a selective and sensitive probe for the colorimetric detection of cysteine.* Analytical Methods, 2012. **4**(6): p. 1747-1752.
18. Li, L. and B. Li, *Sensitive and selective detection of cysteine using gold nanoparticles as colorimetric probes.* Analyst, 2009. **134**(7): p. 1361-1365.
19. Ravindran, A., et al., *Selective colorimetric sensing of cysteine in aqueous solutions using silver nanoparticles in the presence of Cr 3+.* Talanta, 2011. **85**(1): p. 533-540.
20. Han, C., et al., *Colorimetric sensing of cysteine using label-free silver nanoparticles.* Sensors and Actuators B: Chemical, 2014. **202**: p. 574-582.
21. Chetty, A., et al., *Hydroxyapatite: synthesis, properties, and applications.* Polymers and composites, Materials science and manufacturing, 2013.

22. Koutsopoulos, S., *Synthesis and characterization of hydroxyapatite crystals: a review study on the analytical methods.* Journal of biomedical materials research, 2002. **62**(4): p. 600-612.

23. Lu, X., et al., *Hexagonal hydroxyapatite formation on TiO2 nanotubes under urea modulation.* CrystEngComm, 2011. **13**(11): p. 3741-3749.

24. Okada, M. and T. Matsumoto, *Synthesis and modification of apatite nanoparticles for use in dental and medical applications.* Japanese Dental Science Review, 2015. **51**(4): p. 85-95.

25. Liu, X., P.K. Chu, and C. Ding, *Surface modification of titanium, titanium alloys, and related materials for biomedical applications.* Materials Science and Engineering: R: Reports, 2004. **47**(3): p. 49-121.

26. Santos, I.M.G.d., et al., *Crystallographic Aspects Regarding the Insertion of Ag+ Ions into a Hydroxyapatite Structure.* Materials Research, 2015. **18**(4): p. 881-890.

27. Park, S., et al., *Removal of cadmium and lead from aqueous solution by hydroxyapatite/chitosan hybrid fibrous sorbent: kinetics and equilibrium studies.* Journal of Chemistry, 2015. **2015**.

28. Mousa, S., N. Ammar, and H. Ibrahim, *Removal of lead ions using hydroxyapatite nano-material prepared from phosphogypsum waste.* Journal of Saudi Chemical Society, 2016. **20**(3): p. 357-365.

29. Kusrini, E., et al. *Removal of Heavy Metals from Aqueous Solution by Hydroxyapatite/Chitosan Composite*. in *Advanced Materials Research*. 2013. Trans Tech Publ.

30. Kim, W., et al., *Removal of Cu (II) with hydroxyapatite (animal bone) as an inorganic ion exchanger.* Desalination and Water Treatment, 2009. **4**(1-3): p. 269-273.

31. Yan Li, D.W., and Sierin Lim, *Fabrication and Applications of Metal-Ion-Doped Hydroxyapatite Nanoparticles.* Juniper Online Journal Material Science (JOJMS) 2017. **1**(2): p. 1-6.

32. Feng, Q.L., et al., *Antibacterial effects of Ag-HAp thin films on alumina substrates.* Thin Solid Films, 1998. **335**(1): p. 214-219.

33. Guzman Vazquez, C., C. Pina Barba, and N. Munguia, *Stoichiometric hydroxyapatite obtained by precipitation and sol gel processes.* Revista mexicana de física, 2005. **51**(3): p. 284-293.

34. Agrawal, K., et al., *Synthesis and characterization of hydroxyapatite powder by sol-gel method for biomedical application.* Journal of Minerals and Materials Characterization and Engineering, 2011. **10**(08): p. 727.

35. Ciobanu, G., S. Ilisei, and C. Luca, *Hydroxyapatite-silver nanoparticles coatings on porous polyurethane scaffold.* Materials Science and Engineering: C, 2014. **35**: p. 36-42.

36. Jafari, S. and K. Adibkia, *Application of hydroxyapatite nanoparticle in the drug delivery systems.* J Mol Pharm Org Process Res, 2015. **3**: p. 1-2.

37. Abidi, S.S.A. and Q. Murtaza, *Synthesis and characterization of nano-hydroxyapatite powder using wet chemical precipitation reaction.* Journal of Materials Science & Technology, 2014. **30**(4): p. 307-310.

38. Laonapakul, T., *Synthesis of hydroxyapatite from biogenic wastes.* KKU Engineering Journal, 2015. **42**(3): p. 269-275.

39. Elkabouss, K., et al., *Cobalt-exchanged hydroxyapatite catalysts: magnetic studies, spectroscopic investigations, performance in 2-butanol and ethane oxidative dehydrogenations.* Journal of Catalysis, 2004. **226**(1): p. 16-24.

40. Andrade, F.A.C., et al., *Preparation, characterization and antibacterial properties of silver nanoparticles–hydroxyapatite composites by a simple and eco-friendly method.* Ceramics international, 2016. **42**(2): p. 2271-2280.

41. Dey, P.K.B.a.S., *Effects and Applications of Silver Nanoparticles in different Field.* International Journal of Recent Scientific Research, 2015. **6**(8): p. 5880-583.

42. Gonzalez, A. and C. Noguez, *Optical properties of silver nanoparticles.* physica status solidi (c), 2007. **4**(11): p. 4118-4126.

43. Xu, X., et al., *Fabrication and robotization of ultrasensitive plasmonic nanosensors for molecule detection with Raman scattering.* Sensors, 2015. **15**(5): p. 10422-10451.

44. Prabhu, S. and E.K. Poulose, *Silver nanoparticles: mechanism of antimicrobial action, synthesis, medical applications, and toxicity effects.* International Nano Letters, 2012. **2**(1): p. 32.

45. Ku**ś**mierek, K., et al., *Ultraviolet derivatization of low-molecular-mass thiols for high performance liquid chromatography and capillary electrophoresis analysis.* Journal of Chromatography B, 2011. **879**(17): p. 1290-1307.

46. Lambeth, D.O., et al., *Implications for in vitro studies of the autoxidation of ferrous ion and the iron-catalyzed autoxidation of dithiothreitol.* Biochimica et Biophysica Acta (BBA)-General Subjects, 1982. **719**(3): p. 501-508.

47. Isokawa, M., et al., *Analytical methods involving separation techniques for determination of low-molecular-weight biothiols in human plasma and blood.* Journal of Chromatography B, 2014. **964**: p. 103-115.

48. Grant, G.A., *Modification of cysteine.* Current Protocols in Protein Science, 2017: p. 15.1. 1-15.1. 23.

49. Alchin, D., *Ion exchange resins.* Chemical processes in New Zealand. New Zealand Institute of Chemistry Education, pp XIII-D-1–XIII-D-7, 1998.

50. Ruamaram, S., *Determination of Urinary Glucose by Fluorescence Spectroscopy of Curcumin using Fenton Reaction*, in *Chemistry*. 2015, Chulalongkorn University: Bangkok, Thailand. p. 23.

51. *AOAC Official Methods of Analysis, Appendix F: Guidelines for standard method performance requirements, 2016*. [cited 2017 1 september]; Available from: http://www.eoma.aoac.org/app_f.pdf.

52. Lu, X., et al., *Nano-Ag-loaded hydroxyapatite coatings on titanium surfaces by electrochemical deposition.* Journal of the Royal Society Interface, 2011. **8**(57): p. 529-539.

APPENDIX

VITA

Miss Retno Prasetia was born on January 18, 1992 in Samarinda, Indonesia. She received a Bachelor's degree of Education in Chemistry from Mulawarman University, East Borneo, in 2013. After graduated, she joined SEAMEO, QITEP in Science working as Fresh graduate for improving skill of teachers and helping them ready for the new curriculum (K-13) that would be implemented from 2013. Six-month afterwards, she joined Bridging Program from Mulawarman University to improve some skills before study abroad. In 2015, She has been a graduate student at Department of Chemistry, Chulalongkorn University under supervision of Assistant Professor Dr. Fuangfa Unob. In February 2017, she received a proceeding of the Pure and Applied Chemistry International Conference 2017 (PACCON 2017), the Chemical Society of Thailand (CST) and Organizing University (KMUTNB) which was held on February 2 - 3, 2017 at Centra Government Complex Hotel & Convention Center Chaeng Watthana, Bangkok, Thailand. She then completed her Master degree of Science in 2017.